Journal of Fluorine Chemistry 130 (2009) 870–877

Contents lists available at ScienceDirect

Journal of Fluorine Chemistry

journal homepage: www.elsevier.com/locate/fluor

Bonding strength of fluorinated and hydrogenated surfactant to bovine serum albumin

Ling Li [a], Yingxi Wang [a], Gongwu Song [a], Shuilin Wu [a,b], Paul K. Chu [b], Zushun Xu [a,b,*]

[a] Ministry-of-Education Key Laboratory for the Synthesis and Application of Organic Function Molecules, Hubei University, Wuhan 430062, China
[b] Department of Physics & Materials Science, City University of Hong Kong, Tat Chee Avenue, Kowloon, Hong Kong, China

ARTICLE INFO

Article history:
Received 21 April 2009
Received in revised form 7 June 2009
Accepted 25 June 2009
Available online 8 July 2009

Keywords:
Fluorinated/hydrogenated surfactant
BSA
Quenching
Energy transfer
Interaction

ABSTRACT

The interactions between bovine serum albumin (BSA) and different surfactants are investigated by the fluorescence technique. Pairs of fluorinated and hydrogenated surfactants with similar hydrophobic chain lengths including potassium perfluorooctanesulfonate and sodium octanesulfonate are studied in order to determine their interactions with BSA. The binding constants and thermodynamic parameters between BSA and different surfactants are compared and the main binding strength is determined. The mechanism of quenching and change of particle size gives rise to the binding force. Based on the FRET theory, the distances between potassium perfluorooctanesulfonate/sodium octanesulfonate and BSA are calculated and it is found that the fluorinated surfactant exhibits stronger interactions with proteins than the hydrogenated one, which is also proved by zeta potential and TEM.

© 2009 Elsevier B.V. All rights reserved.

1. Introduction

Surfactants which are amphipathic substances composed of both hydrophilic and hydrophobic groups are widely used in inducing unfolding of proteins and in some special cases, stabilizing proteins at very low concentrations [1]. Proteins undergo changes in their natural state by interacting with different surfactants which are used as adsorbates in order to control the hydrophobic–hydrophilic characteristics of the protein surface [2]. Determination of the structural and thermodynamic response of proteins under various solvent conditions is one of the ways to elucidate their stability, folding pathway, and intermolecular aggregation behavior [3]. Systematic studies of interactions between proteins and surfactants are necessary from the viewpoint of both fundamental understanding and applications.

Surfactants are used to extract proteins from cell membranes. Surfactant–protein interactions are comparable to some extent to lipid–protein interactions in the membranes of living cells [3,4] and can account for the transport of metabolites in body fluids [5,6]. Previous studies have focused on conventional surfactants usually containing a hydrophobic hydrocarbon group, so-called hydrogenated surfactants or hydrocarbon surfactants. There is another class of special surfactants, fluorinated surfactants or fluorocarbon surfactants, in which interactions with proteins have rarely been studied. In fluorinated surfactants, the hydrogen atoms in the hydrophobic tails are replaced by fluorine ones. A better understanding of the interactions between fluorinated surfactants used in pharmaceutical, cosmetic, biological, and medical applications and proteins is required [7–9]. Therefore, it is of interest to compare the differences in the interactions between hydrogenated and fluorinated surfactants and proteins, but so far, fluorescence spectroscopy has seldom been utilized in this regard.

In the work reported here, fluorescence spectroscopy is employed to analyze the difference in the bonding strength. This piece of work aims at obtaining experimental results to compare the different interactions between fluorinated/hydrogenated surfactants and proteins. Here, potassium perfluorooctanesulfonate (PFOS) and sodium octanesulfonate (SOS) are used as the fluorinated surfactant and hydrogenated surfactant, respectively. Serum albumins which are the most abundant proteins in blood plasma are one of the most extensively studied proteins and the major soluble protein constituents in the circulatory system. They play a dominant role in the transport and deposition of endogenous and exogenous ligands in blood, as serum albumins often enhance the apparent solubility of hydrophobic drugs in plasma and modulate their delivery to cells *in vivo* and *in vitro* [10]. In this work, bovine serum albumin (BSA) is selected as the protein model due to its medical importance, low cost, ready availability, and ligand-binding properties.

* Corresponding author at: Ministry-of-Education Key Laboratory for the Synthesis and Application of Organic Function Molecules, Hubei University, Wuhan 430062, China. Tel.: +86 2761120608.
E-mail addresses: zushunxu@hubu.edu.cn, waitingll@yahoo.com (Z. Xu).

0022-1139/$ – see front matter © 2009 Elsevier B.V. All rights reserved.
doi:10.1016/j.jfluchem.2009.06.025

2. Results and discussion

2.1. Fluorescence characteristics of BSA

Fluorescence quenching refers to a process in which the fluorescence intensity from a sample diminishes. A variety of molecular interactions can result in quenching and they include excited-state reactions, molecular rearrangements, energy transfer, ground-state complex formation, and collisional quenching. In collisional quenching, the intensity reduction is described by the well-known Stern–Volmer equation [11]:

$$\frac{F_0}{F} = 1 + K_{SV}[Q], \quad (1)$$

where F_0 and F are the steady-state fluorescence intensities with and without the quencher, K_{SV} is the Stern–Volmer quenching constant, and [Q] is the quencher concentration. Fig. 1(a) shows the emission spectra of BSA in the presence of various concentrations of SOS. It can be observed that the fluorescence intensity of BSA decreases regularly with increasing of SOS concentration. Fig. 1(b) depicts the emission spectra of BSA in the presence of various concentrations of PFOS. The fluorescence intensities of BSA diminish regularly with increasing PFOS concentrations.

Fig. 2(a) illustrates that at low concentrations, the results (real line) agree very well with the Stern–Volmer equation, but at high concentrations, the results deviate from the initial linearity. In order to avoid the inner filter effects [6] and discuss the results within the linear concentration range, we carry out the experiments within the linear part of Stern–Volmer dependence (F_0/F against [Q]), and stabilize the concentrations of BSA at 1.5×10^{-6} mol L^{-1} while the concentrations of SOS are varied from 1.0×10^{-5} to 5.0×10^{-5} mol L^{-1}. Fig. 2(b) shows that at low concentrations, the results agree well with the Stern–Volmer equation. We also stabilize the concentrations of BSA at 1.0×10^{-6} mol L^{-1} and the concentrations of PFOS are changed from 0.5×10^{-6} to 3.0×10^{-6} mol L^{-1} in order to discuss the results within the linear concentration range.

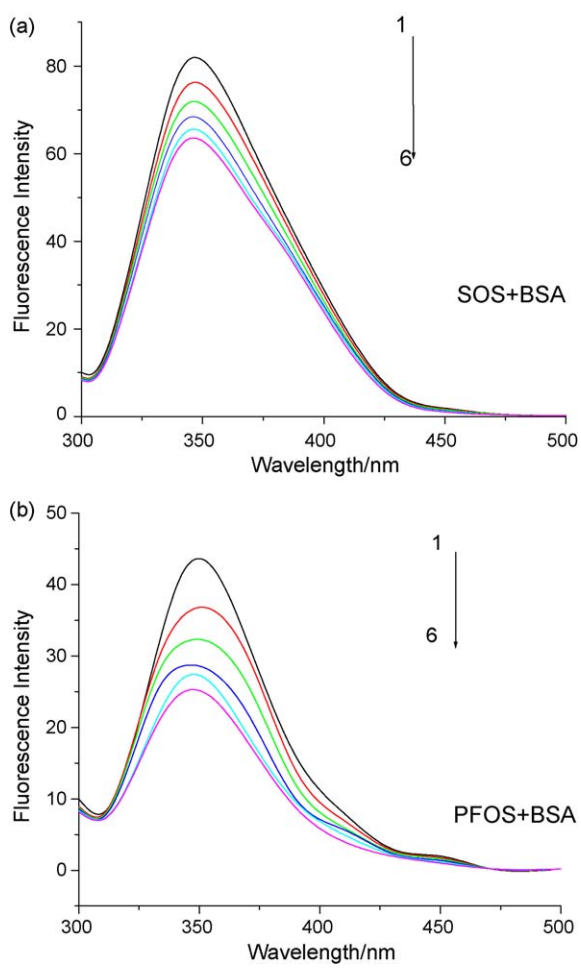

Fig. 1. Emission spectra of surfactant–BSA system with surfactants concentrations: (a) C_{BSA}: 1.5×10^{-6} mol L^{-1}; C_{SOS} (1–6): 0.000, 1.0×10^{-5}, 2.0×10^{-5}, 3.0×10^{-5}, 4.0×10^{-5}, 5.0×10^{-5} mol L^{-1}; (b) C_{BSA}: 1.0×10^{-6} mol L^{-1}; C_{PFOS} (1–6): 0.000, 0.5×10^{-6}, 1.0×10^{-6}, 1.5×10^{-6}, 2.0×10^{-6}, 3.0×10^{-6} mol L^{-1}.

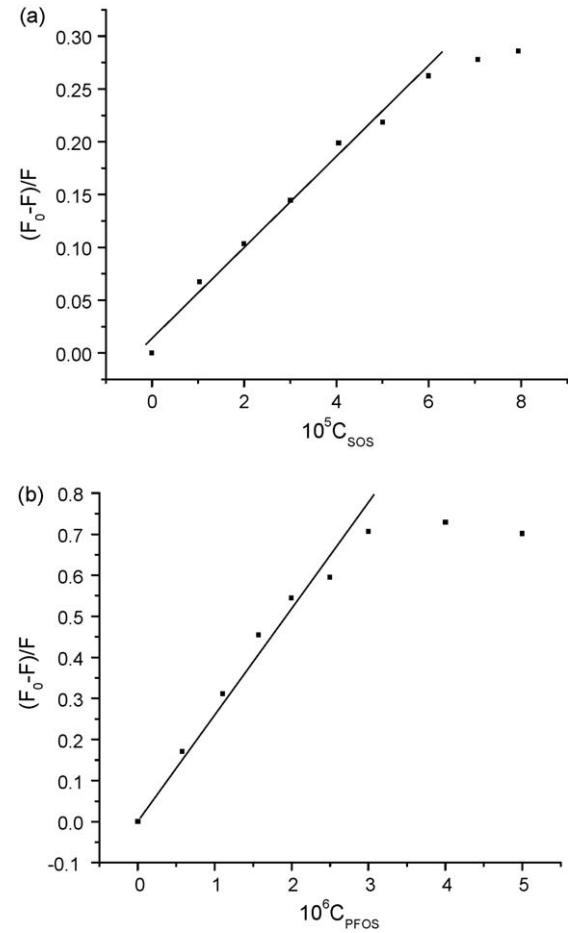

Fig. 2. Fluorescence intensity of the surfactant–BSA system with surfactants concentrations: (a) C_{BSA}: 1.5×10^{-6} mol L^{-1}; (b) C_{BSA}: 1.0×10^{-6} mol L^{-1}.

Both surfactants cause obvious reduction in the BSA fluorescence intensity, and the PFOS concentration is lower than that of SOS. The concentration of PFOS is only allowed in a relatively low concentration range from 0.5×10^{-6} to 3.0×10^{-6} mol L^{-1}. The phenomena may be explained by the decrease of the critical micelle concentration which influences surfactant binding to BSA. Fig. 3 plots the conductivity versus surfactant concentrations. The location of the inflexion point is considered to be the critical micell concentration (CMC) of the micelles. It is obvious that the CMCs of PFOS and SOS are 2.03×10^{-4} and 0.0139 mol L^{-1}, respectively. In the fluorinated surfactant, substitution of the larger and highly electronegative fluorine atom for the smaller hydrogen increases the amphiphilic nature of the surfactant and lowers the surface tension and critical micelle concentration [3]. Hence, the CMC of PFOS is much lower than that of SOS. In order to discuss the binding mechanism exactly, all surfactants concentration are lower than CMC so that each surfactant in the solution is monomer.

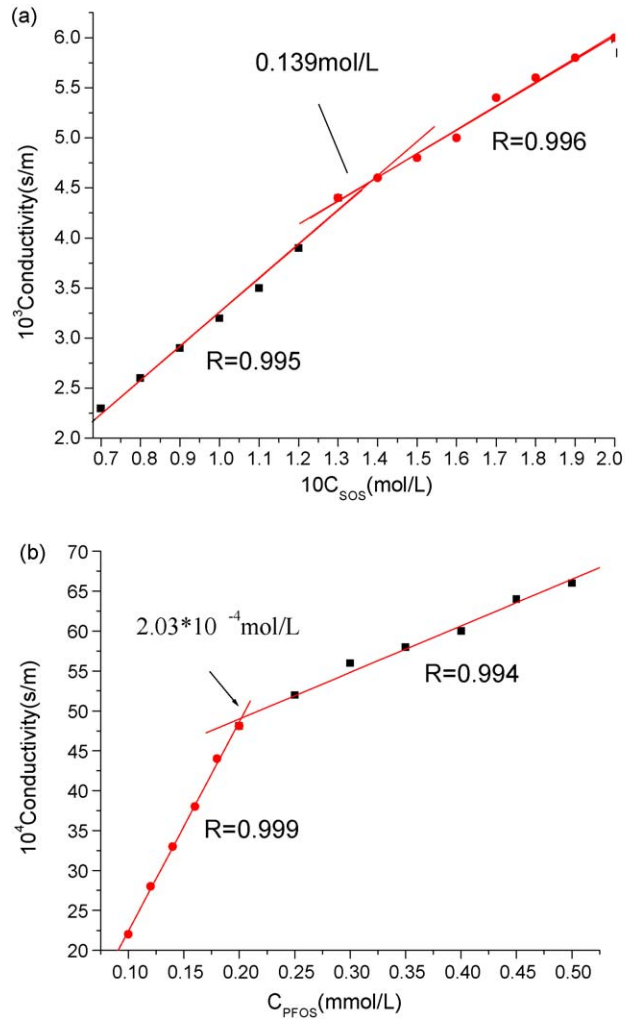

Fig. 3. Electrical conductivity of surfactants: (a) SOS; (b) PFOS.

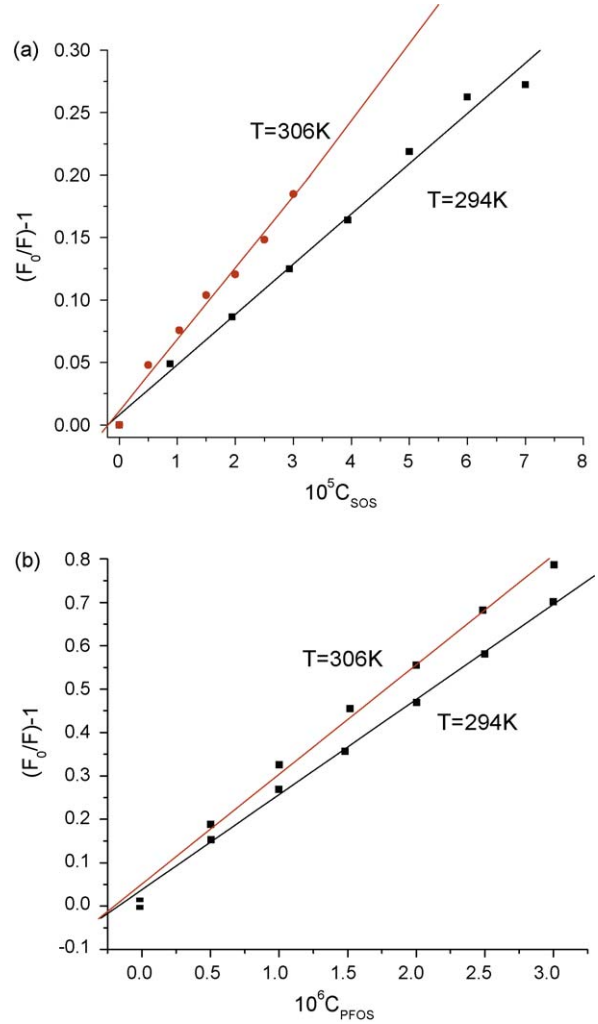

Fig. 4. Stern–Volmer plot at different temperatures: (a) C_{BSA}: 1.5×10^{-6} mol L^{-1}; (b) C_{BSA}: 1.0×10^{-6} mol L^{-1}.

Quenching can occur via different mechanisms which are usually classified as dynamic quenching and static quenching. Dynamic and static quenching can be distinguished by their different dependence on temperature and excited-state lifetime. Higher temperatures result in faster diffusion and consequently more substantial collisional quenching. A higher temperature typically results in the dissociation of weakly bound complexes and thus less static quenching [12].

Fig. 4 displays the Stern–Volmer plots of the quenching of BSA fluorescence by SOS and PFOS at different temperatures. The corresponding Stern–Volmer quenching constants at different temperatures are shown in Table 1. The results indicate that the probable quenching mechanism of fluorescence of BSA by SOS is a dynamic one because the K_{SV} value increases with temperature [13]. Similarly, the probable quenching mechanism of fluorescence of BSA by PFOS is dynamic because of increasing K_{SV} with higher temperature.

Table 1
Stern–Volmer quenching constant K_{SV} and relative thermodynamic parameters.

Surfactant	T (K)	K_{SV} (L mol^{-1})	R	ΔH (kJ mol^{-1})	ΔS (J mol^{-1} K^{-1})	ΔG (kJ mol^{-1})
SOS	294	4.06×10^3	0.9954	22.78	147.09	−20.17
	306	5.71×10^3	0.9922			−21.79
PFOS	294	2.17×10^5	0.9984	6.19	122.89	−29.98
	306	2.30×10^5	0.9967			−31.35

R is the linear quotient.

Table 1 shows that the Stern–Volmer quenching constant K_{SV} of PFOS is much larger than that of SOS at the same temperature. It can be concluded that PFOS has stronger binding to BSA than SOS. The rigidity of the C–F bond stiffens the perfluoroalkanoate chain and strengthens the binding to other molecules [3].

2.2. Thermodynamic parameters and nature of the binding forces

The binding forces between the surfactant and BSA usually include nonspecific hydrophobic interactions and specific electrostatic interactions [14]. The Stern–Volmer quenching constants of BSA are measured at 294 and 306 K. If the enthalpy change (ΔH) does not vary significantly over the temperature range, its value and that of entropy change (ΔS) can be determined from the van't Hoff equation:

$$\ln K = -\frac{\Delta H}{RT} + \frac{\Delta S}{R}, \quad (2)$$

where the constant K is analogous to the Stern–Volmer quenching constant K_{SV} at the corresponding temperature [15,16]. The free energy change (ΔG) is estimated from the following relationship:

$$\Delta G = \Delta H - T\Delta S, \quad (3)$$

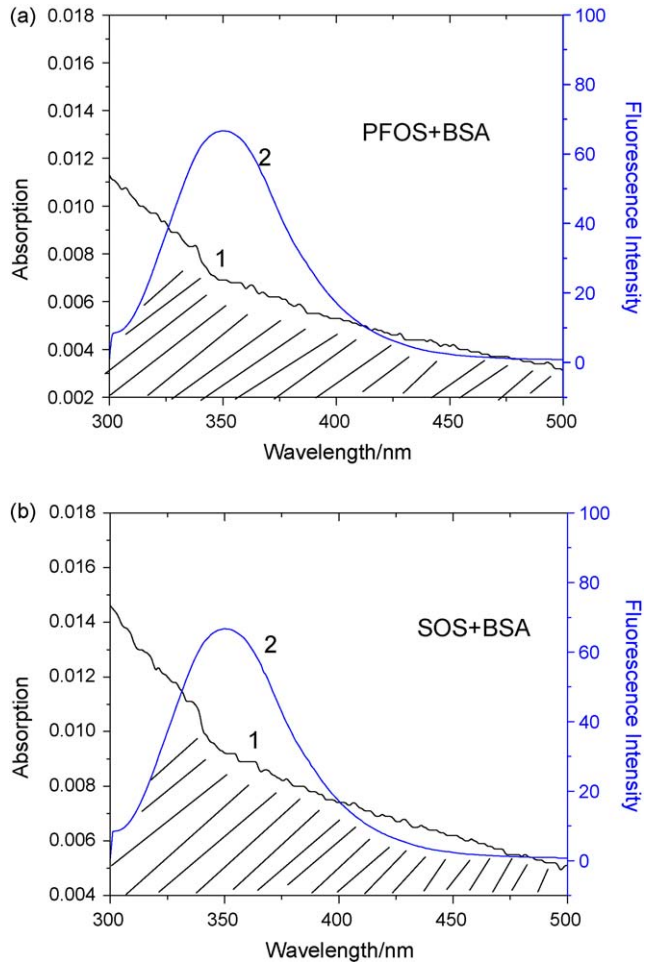

Fig. 5. Spectral overlap of Surfactant absorption (1) with BSA fluorescence (2). (a) $C_{BSA} = C_{SOS} = 3.0 \times 10^{-6}$ mol L^{-1}, (b) $C_{BSA} = C_{PFOS} = 3.0 \times 10^{-6}$ mol L^{-1}.

where ΔH, ΔS, and ΔG are obtained from the above equations and shown in Table 1.

The negative free energy (ΔG) means that the interaction process is spontaneous. The positive enthalpy (ΔH) and entropy (ΔS) values indicate that the hydrophobic force plays a major role in the binding [17]. This may be the main reason that PFOS exhibits stronger interactions with BSA than SOS. Fluorine atoms enhance the hydrophobic property of the surfactant and hydrophobic force leading to stronger binding.

2.3. Energy transfer from BSA to surfactant

According to the FRET theory [18,19], energy transfer occurs under the following conditions: (i) the donor produces fluorescence light, (ii) the fluorescence emission spectrum of the donor and UV absorption spectrum of the acceptor have more overlap, and (iii) the distance between the donor and acceptor is less than 8 nm. The energy transfer effect is related to not only to the distance between the acceptor and donor, but also the critical energy transfer distance. The relationship between these factors is:

$$E = 1 - \left(\frac{F}{F_0}\right) = \frac{R_0^6}{R_0^6 + r^6}, \quad (4)$$

where r is the distance between the donor and acceptor [20] and R_0 is the critical distance when the efficiency of transfer is 50%.

$$R_0^6 = 8.79 \times 10^{-25} K^2 n^{-4} \Phi J. \quad (5)$$

Table 2
Energy transfer parameters.

Donor	Acceptor	R_0 (nm)	r (nm)	E
BSA	SOS	5.94	7.56	19.05%
BSA	PFOS	5.90	7.50	19.16%

In Eq. (5), K^2 is the spatial orientation factor of the dipole, n is the index of refraction of the medium, Φ is the fluorescence quantum yield of the donor, and J is the overlap integral of the fluorescence emission spectra of the donor and the absorption spectra of the acceptor, which can be calculated by the following equation:

$$J = \frac{\sum F(\lambda)\varepsilon(\lambda)\lambda^4 \Delta\lambda}{\sum F(\lambda)\Delta\lambda}, \quad (6)$$

in which $F(\lambda)$ is the corrected fluorescence intensity of the donor in the wavelength range (λ to $\Delta\lambda$) and $\varepsilon(\lambda)$ is the extinction coefficient of the acceptor at λ.

The overlapping between the absorption spectra of SOS and fluorescence spectra of BSA (SOS:BSA = 1:1) are shown in Fig. 5(a) and the overlapping spectra between the absorption spectra of PFOS and fluorescence spectra of BSA (PFOS:BSA = 1:1) are displayed in Fig. 5(b). Due to the good overlap between the emission spectrum of BSA and the absorption spectrum of each surfactant, nonradiative energy transfer between them is possible. Hence, J can be evaluated by integrating the spectra in Fig. 4 for λ = 300–500 nm. Under these experimental conditions, R_0, r, and E can be calculated by using $K^2 = 2/3$, $n = 1.36$, and $\Phi = 0.15$ [21] according to Eqs. (4)–(6). The results are summarized in Table 2.

The data of r for SOS is 7.56 nm which is in the range (<8 nm) [22], illustrating that nonradiative energy transfer occurs between both SOS and BSA. Similarly, the data of r for PFOS is 7.50 nm, implying that energy transfer occurs between both PFOS and BSA. However, the distance r of PFOS is closer than that of SOS and it can also be explained by the stronger interaction between PFOS and BSA.

2.4. Particle size of surfactants interaction with BSA

Fig. 6(a) and (b) shows the changes in the particle size of BSA with different SOS concentrations and different PFOS concentrations at their critical micell concentration, respectively. Fig. 6(a) shows that the particle diameters decrease and then increase with increasing SOS concentrations. It may be explained by that the SOS ions bind to groups of opposite charges on the protein until saturation inducing protein aggregation [23] and the particle size decreases. After the electrostatically absorbed SOS causes the protein to expand, BSA is accessible to the surfactant by means of hydrophobic interactions and consequently, the particle size increases. Fig. 6(b) shows the same results. Therefore, at low concentrations, the main binding force is electrostatic resulting in the small particle diameter, whereas at relative high concentrations, the main binding force is hydrophobic resulting in larger particle sizes.

2.5. Zeta potential of surfactants interaction with BSA

Fig. 7(a) and (b) shows the zeta potential of the interaction between BSA and the surfactants SOS and PFOS as a function of surfactant concentration at the temperature of 25 °C. As the protein charge is usually low, and electrophoresis is carried out at normal ionic strength, the zeta potential of such a particle can be expected to be low and negative zeta potential values can be observed. It is clear that the negative zeta potential value becomes

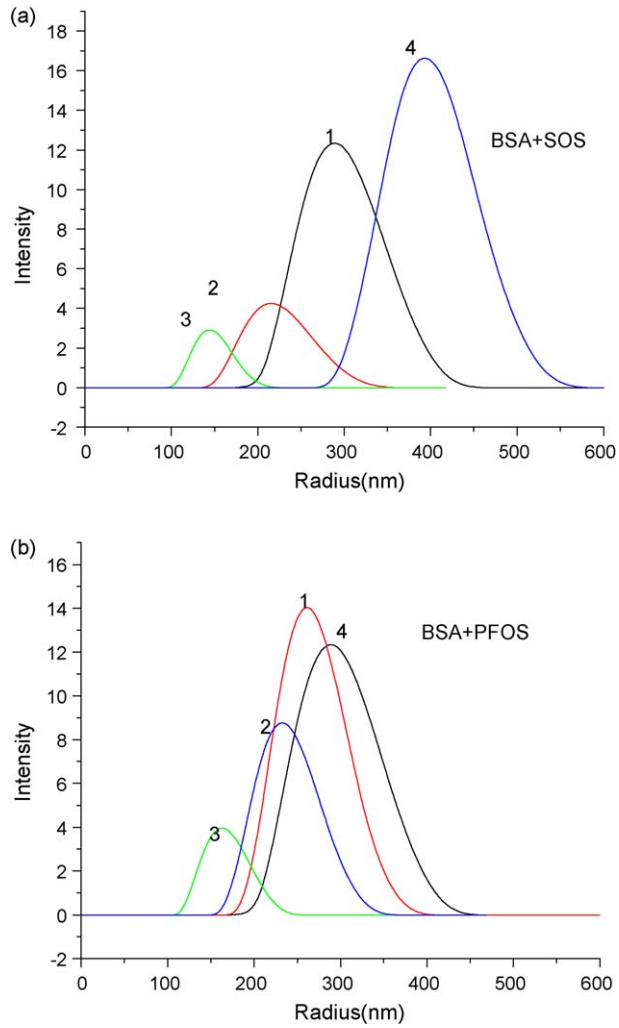

Fig. 6. Particle size distribution for a fixed BSA concentration: (a) C_{SOS} (1–6): 0.000, 1.0×10^{-5}, 2.0×10^{-5}, 3.0×10^{-5}, 4.0×10^{-5}, 5.0×10^{-5} mol· L^{-1}; (b) C_{PFOS} (1–6): 0.000, 0.5×10^{-6}, 1.0×10^{-6}, 1.5×10^{-6}, 2.0×10^{-6}, 3.0×10^{-6} mol L^{-1}; BSA: 1.2×10^{-5} mol L^{-1}.

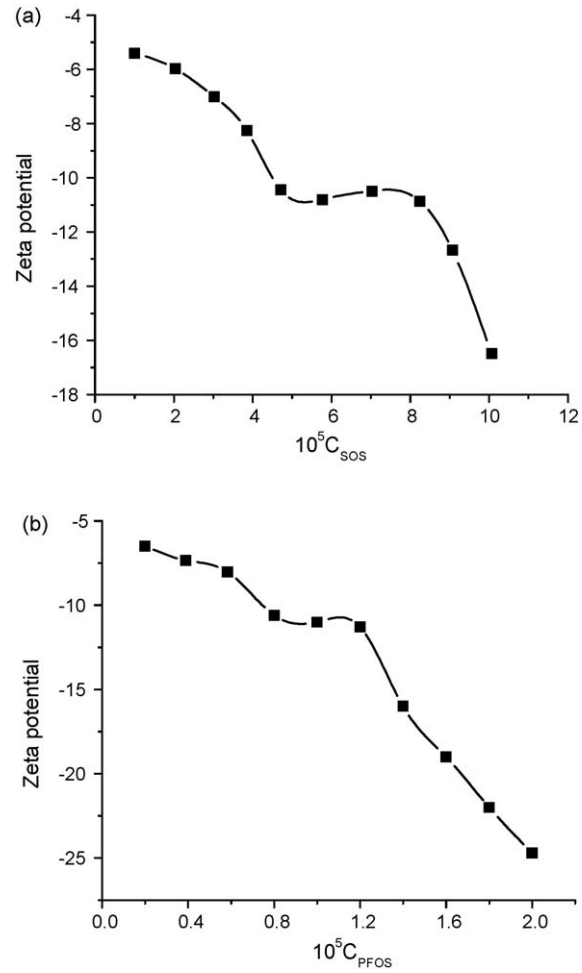

Fig. 7. Zeta potential of surfactant–BSA system with surfactants concentrations: (a) SOS; (b) PFOS; BSA: 1.6×10^{-6} mol L^{-1}.

more negative as the surfactant concentration increase. This negative value of the zeta potential suggests that hydrophobic interaction is predominant [3].

In the interaction with SOS, there is an initial slightly decrease of the zeta potential, which tends to a plateau, after that there is an abrupt decrease, the zeta potential becomes more negative and reaches minimum. It can be concluded that at low concentrations, the main binding force is electrostatic. The zeta potential of BSA are gradually negative affected by anionic surfactant SOS through electrostatic interaction. When SOS ions bind to groups of opposite charges on the protein until saturation, the zeta potential reaches a plateau. After that, at relative high concentrations, the main binding force is hydrophobic. The zeta potential of BSA are dramatically negative because of the aggregation of SOS through hydrophobic interaction.

In the interaction with PFOS, a similar phenomenon has been observed. At low concentrations, the main binding force is electrostatic. The zeta potential of BSA slightly decrease because of the adsorption of anionic surfactant PFOS on BSA through electrostatic interaction. When PFOS ions bind to groups of opposite charges on the protein until saturation, the zeta potential nearly keeps a constant. After that, at relative high concentrations, the main binding force is hydrophobic. The zeta potential of BSA dramatically decrease because of the aggregation of PFOS through hydrophobic interaction. The conclusions are in accordance with that concluded from particle size.

Furthermore, when the main binding force is hydrophobic, the dramatically decrease of zeta potential in PFOS–BSA system is much more negative than that in SOS–BSA system. It can be explained that PFOS has stronger hydrophobic interactions with BSA than SOS for the higher hydrophobicity of fluorine atoms.

2.6. TEM micrographs of surfactants binding to BSA

Fig. 8(a) exhibits the TEM images of SOS surfactants binding to BSA with different SOS concentrations in aqueous solution. Fig. 8(a) shows the monomer of SOS is rod-like molecule, and with increasing concentration, the rod-like molecules become dense (1 and 2). It can be seen that "necklace" structure is formed when BSA is added (3), and when the concentration of SOS is higher, the "pearl necklace" structure of SOS binding to BSA is very clear (4). The phenomena can be explained that the aggregation of SOS on BSA through hydrophobic interaction, and aggregates form "pearl necklace" structure with BSA as chain and SOS molecules as pearls.

Fig. 8(b) shows TEM images of PFOS binding to BSA with different PFOS concentrations in aqueous solution. It shows PFOS forms core–shell structure, and with increasing concentration, the core–shell spheres become dense (5 and 6). In fact, the concentration of PFOS is much lower than SOS and much lower than the CMC of PFOS, but PFOS forms a core–shell structure because of strong hydrophobic characteristic of PFOS. After

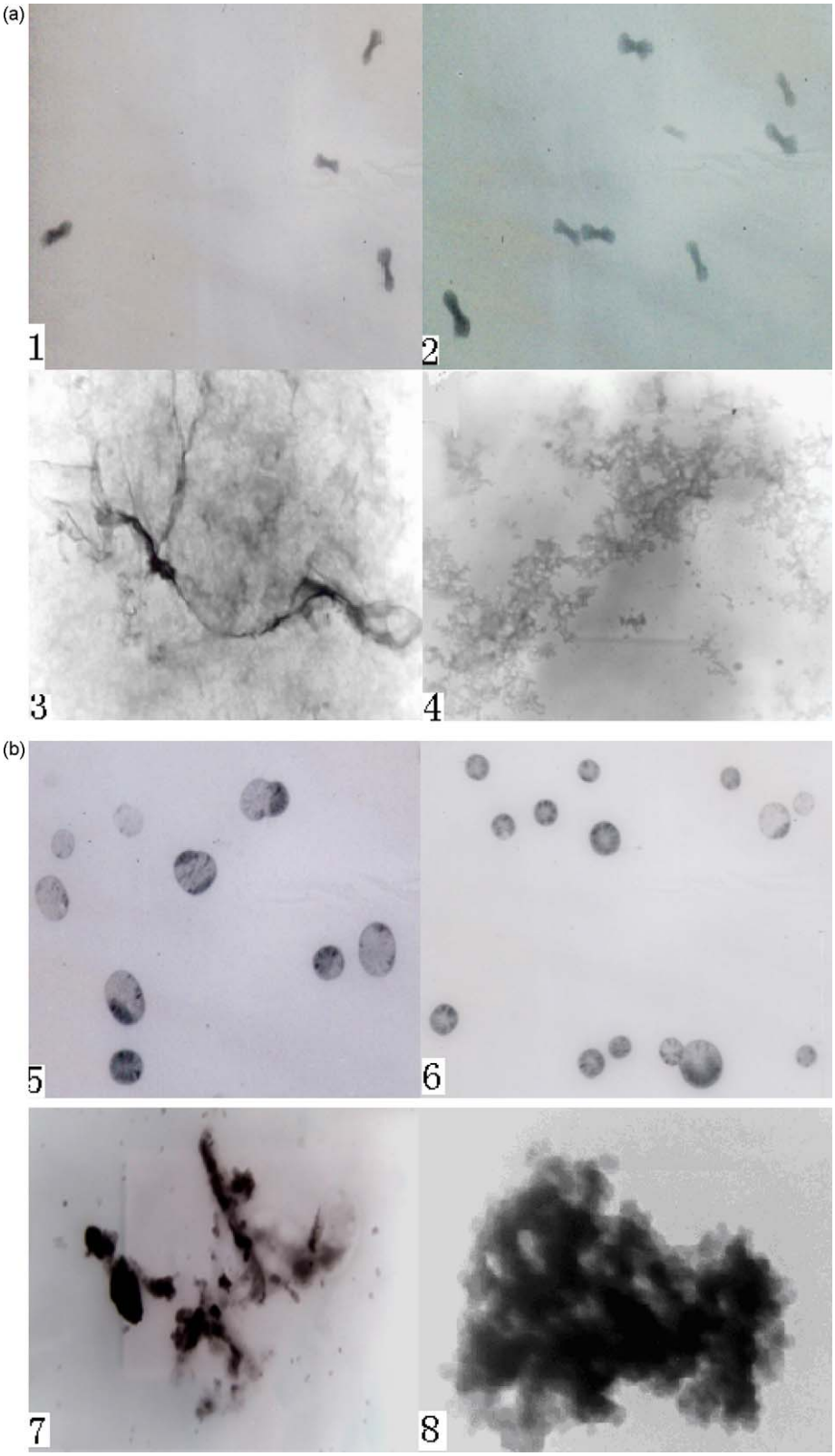

Fig. 8. TEM micrographs of surfactants binding to BSA. (a) C_{SOS} (1–4): 2.0×10^{-6}, 4.0×10^{-6}, 2.0×10^{-6}, 4.0×10^{-6} mol L^{-1}; C_{BSA} (1–4): 0.0, 1.0×10^{-6}, 1.0×10^{-6} mol L^{-1}; (b) C_{PFOS} (5–8): 1.0×10^{-6}, 2.0×10^{-6}, 1.0×10^{-6}, 2.0×10^{-6} mol L^{-1}; C_{BSA} (5–8): 0.0, 1.0×10^{-6}, 1.0×10^{-6} mol L^{-1}.

evaporation of the solvent water, the concentration of PFOS becomes much higher than that in solution. Because of the strong hydrophobic characteristic of PFOS, PFOS has a high tendency to form micell, so the core–shell sphere can be observed (5). When the concentration of PFOS is higher, forming micell is more easy, so we can observe that the spheres are more and they are more close to each other, which tends to form a bigger sphere (6). Because of the hydrophobic fluorine atoms, during the self-assembly process, PFOS has a high tendency to bury themselves in the interior of the micelles thereby forming the core–shell structure.

After BSA is added to PFOS solution, we can see the "pearl necklace" structure is forming (7), and some spheres are coming close to "pearl necklace". Comparing with Fig. 8(a, 3), the "pearl necklace" is more clear and the "pears" are more dense. It exposes that PFOS has more hydrophobic nature than SOS, so the aggregation of PFOS on BSA is more easy. When the concentration of PFOS is increasing, more "pearls" aggregation on "necklace" and cluster structure is formed. So aggregation is more easy when surfactant concentration is more high or surfactant is more hydrophobic.

Therefore, Fig. 8 proves that PFOS has more hydrophobic interaction with BSA than SOS.

3. Experimental

3.1. Apparatus

The fluorescence spectra and the intensity of fluorescence were measured on a Shimadzu RF-540 spectrofluorometer (Kyoto, Japan). The absorption spectra were acquired using a PerkinElmer λ17 UV–VIS spectrophotometer (P-E Co., America). A WH-2 vortex mixer (Huxi Instrumental Co., Shanghai, China) was used to blend the solution. A high performance particle sizer (Malvern, America) was employed to measure the particle size. Nano-ZS ZEN3600 (Malvern Instruments, US). Transmission electron microscopy (TEM) micrographs were obtained by JEM-100SX electron microscope (JEOL, Japan).

3.2. Reagents

All the reagents were of analytical-reagent grade and made in China. The concentrations of potassium perfluorooctanesulfonate and sodium octanesulfonate were both 1.0×10^{-4} mol L^{-1}. The stock solution of BSA was prepared by dissolving commercial BSA (Sino-American biotechnology company, China,) in doubly distilled water at 0–4 °C. The concentration of the bovine serum albumin was 2.5×10^{-5} mol L^{-1}. Doubly distilled water was used throughout the experiments.

3.3. Fluorescence spectra

Appropriate solutions of bovine serum albumin and surfactant were added to a 25 mL volumetric flask. The mixture was diluted to 10 mL with doubly distilled water and vortexes. The fluorescence quenching spectra were measured at an excitation wavelength of 290 nm scanned within a wavelength range of 300–500 nm. The fluorescence intensity was measured at the maximum wavelength 350 nm. Both the excitation and emission slits were 10 nm.

3.4. Zeta potential

Zeta potentials measurements of protein–surfactant complex were made using a Nano-ZS ZEN3600 (Malvern, US) by taking the average of five measurements at the stationary level at 25 °C. The cell used was a 5 mm × 2 mm rectangular quartz capillary.

3.5. Transmission electron microscopy (TEM)

The morphology of surfactants and the morphology of their binding to BSA were characterized by TEM (JEOL, Japan). The samples were stained with phosphotungstic acid, and a drop of the samples (concentrations of surfactants solution were lower than CMC) was placed on a Formvar-coated copper grid which was dried in air. The TEM images were obtained at 25 °C at an electron acceleration voltage of 120 kV.

4. Conclusion

The binding of protein to fluorinated surfactant PFOS and hydrogenated surfactant SOS has been compared, and our experimental data such as critical micell concentration, Stern–Volmer quenching constant K_{SV}, and the distance between the donor and acceptor show that PFOS has stronger binding. Fluorescence quenching with increasing surfactant concentrations can be explained by the denaturing of BSA. The experimental results also indicate that the probable quenching mechanisms of BSA by PFOS and SOS are both dynamic.

The binding of surfactants to protein is driven by specific ionic interactions between the surfactant head group and protein as well as by nonspecific hydrophobic interactions [14]. Our experiments reveal that the binding reaction is entropy-driven and the hydrophobic interaction plays a major role in each reaction. For SOS and PFOS as the anionic surfactants, it can be concluded that the driving forces are electrostatic interactions with BSA followed by thermodynamically favorable hydrophobic interactions as evidenced by the negative binding free energy and positive entropy. The change in the particle size shows that the main binding force is electrostatic when the surfactant concentration is low and the hydrophobic interaction prevails at higher concentrations.

Zeta potential experiments prove hydrophobic interaction is predominant and PFOS has stronger interaction with BSA. TEM micrographs also confirm the conclusion and show the different structures of SOS and PFOS, and pearl necklace mode of surfactants binding to BSA is confirmed.

Our results disclose that the fluorinated surfactant (PFOS) has stronger interactions with proteins than the hydrogenated surfactant (SOS) with a similar hydrophobic chain length. The influence of the surfactant on the protein depends on the molecular structure of the surfactant. In a fluorinated surfactant, the hydrogen atoms in the hydrophobic tail are replaced by fluorine atoms. The fluorinated surfactant has larger and highly electronegative fluorine atoms which enhance the hydrophobic nature, and the rigidity of the C–F bond is able to stiffen the perfluoroalkanoate chain, thereby giving rise to stronger binding. In general, a fluorinated surfactant has stronger hydrophobicity than the hydrogenated one with a similar hydrophobic chain length. In the case that the fluorinated and hydrogenated surfactants have a similar hydrophobic chain length, the hydrophobic interactions are expected to be much stronger in systems with fluorinated surfactants and proteins due to the higher hydrophobicity of fluorine atoms. This work provides better understanding of interactions between proteins and fluorinated surfactants and benefits further development of fluorinated surfactants in biomedical applications.

Acknowledgements

The work was supported by Natural Science Foundation of Hubei Province of China and Ministry-of-Education Key Laboratory for the Synthesis and Application of Organic Functional Molecules and Hong Kong Research Grants Council (RGC) General Research Funds (GRF) No. CityU 112306. The authors are also grateful to the financial support by Innovation Group Foundation and Elitist Foundation of the Provincial Science & Technology Department, Hubei, China.

References

[1] K.P. Ananthapadmanabhan, in: E.D. Goddard, K.P. Ananthapadmanabhan (Eds.), Interactions of Surfactants with Polymers and Proteins, 1st ed., CRC Press, London, 1993.

[2] M.N. Jones, D. Chapman, Micelles, Monolayers and Biomembranes, Wiley-Liss, New York, 1995.
[3] G. Prieto, J. Sabín, J.M. Ruso, A. González-Pérez, F. Sarmiento, Colloids Surf. A: Physicochem. Eng. Aspects 249 (2004) 51–55.
[4] S.J. Singer, G.L. Nicolson, Science 175 (1972) 720–731.
[5] A.L. Lehninger, D.L. Nelson, M.M. Cox, Principles of Biochemistry, CBS Publications, New Delhi, 1987.
[6] T. Peters Jr., Serum Albumin Adv. Protein Chem. 37 (1985) 161–245.
[7] E. Kissa, Fluorinated Surfactants, Synthesis, Properties, Applications, Marcel Dekker Inc., New York, 1994.
[8] E. Kissa, Fluorinated Surfactants and Repellents, Marcel Dekker, Inc., New York, 2001.
[9] J.G. Riess, Chem. Rev. 101 (2001) 2797–2920.
[10] D.C. Carter, J.X. Ho, Adv. Protein Chem. 45 (1994) 153–176.
[11] J.R. Lakowicz, Principles of Fluorescence Spectroscopy, Plenum Press, New York, 1999, pp. 237–265.
[12] Y.J. Hua, Y. Liu, X.S. Shen, X.Y. Fang, S.S. Qu, J. Mol. Struct. 738 (2005) 143–147.
[13] G.Z. Chen, X.Z. Huang, J.G. Xu, Z.Z. Zheng, Z.B. Wang, The Methods of Fluorescence Analysis, 2nd ed., Science Press, Beijing, 1990.
[14] S. De, A. Girigoswami, S. Das, J. Colloid Interface Sci. 285 (2005) 562–573.
[15] R.M. Jones, T.S. Bergstedt, D.W. McBranch, D.G. Whitten, J. Am. Chem. Soc. 123 (2001) 6726–6727.
[16] C.B. Murphy, Y. Zhang, T. Troxler, V. Ferry, J.J. Martin, W.E. Jones, J. Phys. Chem. B 108 (2004) 1537–1543.
[17] P.D. Ross, S. Subramanian, Biochemistry 20 (1981) 3096–3102.
[18] R.M. Clegg, Curr. Opin. Biotechnol. 6 (1995) 103–110.
[19] Y.J. Hu, Y. Liu, R.M. Zhao, J.X. Dong, S.S. Qu, J. Photochem. Photobiol. A 179 (2006) 324–329.
[20] J. Tian, J. Liu, X. Tian, Z. Hu, X. Chen, J. Mol. Struct. 691 (2004) 197–202.
[21] C.Q. Jiang, M.X. Gao, J.X. He, Anal. Chim. Acta 452 (2002) 185–189.
[22] B. Valeur, J.C. Brochon, New Trends in Fluorescence Spectroscopy, Springer, Berlin, 2001.
[23] J.M. Ruso, A.G. Pérez, G. Prieto, F. Sarmiento, Int. J. Biol. Macromol. 33 (2003) 67–73.